Proceedings of COBEM 2005
18th International Congress of Mechanical Engineering
November 6-11, 2005, Ouro Preto, MG

AN EFFICIENT NUMERICAL MODEL FOR ISOTHERMAL AND THERMALLY COUPLED INCOMPRESSIBLE FLOWS

Alexandre Luis Braun
Programa de Pós-Graduação em Engenharia Civil (PPGEC)
Universidade Federal do Rio Grande do Sul (UFRGS)
Av. Osvaldo Aranha, 99 – 3° andar, Porto Alegre, RS, Brasil, CEP 90035-190
allbraun@ig.com.br

Armando Miguel Awruch
Programas de Pós-Graduação em Engenharia Civil (PPGEC) e Mecânica (PROMEC)
Universidade Federal do Rio Grande do Sul (UFRGS)
Av. Osvaldo Aranha, 99 – 3° andar, Porto Alegre, RS, Brasil, CEP 90035-190
awruch@adufrgs.ufrgs.br

Abstract. *In this paper an efficient numerical algorithm for isothermal and non-isothermal incompressible flows simulation is presented. In large scale computations, such as 3-D fluid-structure interaction problems, CPU time and memory savings are essential and then the numerical scheme must be chosen carefully. Moreover, some intrinsic characteristics of flows, such as the presence of turbulence and buoyancy effects for example, may reduce the number of options with respect to the scheme that may be used. It is observed that implicit schemes may be inappropriate for highly unsteady problems and they are usually very expensive methods in terms of memory costs. Semi-implicit schemes are very competitive when flows with low Reynolds numbers are analyzed. However, at higher Reynolds numbers efficiency of semi-implicit schemes is lost owing to turbulence effects (turbulence phenomenon must be simulated with small time steps). Explicit schemes request a minimum amount of memory when they are compared to other schemes. On the other hand, the time step is strongly restricted by the stability condition. Even so, they are yet the best choice when it is compared to implicit or semi-implicit schemes, mainly in real unsteady flows where turbulent regimes are observed. In the present model a Taylor-Galerkin scheme with an explicit-iterative solver for the momentum and energy balance equations is used, reducing considerably the processing time when it is compared to the two-step and the semi-implicit Taylor-Galerkin models. The pressure is solved explicitly with a continuity equation obtained invoking the pseudo-compressibility hypothesis. The turbulence is simulated using Large Eddy Simulation (LES) with the Smagorinsky's sub-grid model. In the non isothermal problem buoyancy forces, obtained from the classical Boussinesq's approximation, are considered. The Finite Element Method (MEF) is employed for the spatial discretization with the eight-node isoparametric hexahedral element and analytical expressions are obtained for the element matrices. Classical examples are presented to validate the numerical model.*

Keywords*: Incompressible Flow, Buoyancy forces, Large Eddy Simulation (LES), Finite Element Method (FEM).*

1. Introduction

In recent years the demand for computational codes to simulate engineering problems have grown considerably. This is owing to advances in numerical methods and computer technology. Moreover, experimental works have been gradually replaced by numerical algorithms that can reproduce the experimental conditions reliably (see, for example, *Braun and Awruch*, 2005). Nevertheless, such problems request a great computational effort in terms of CPU time and memory. Hence, drawbacks of each numerical scheme must be carefully evaluated in order to obtain an efficient code for the case which will be analyzed.

The Taylor-Galerkin scheme in the context of the Finite Element Method (FEM) has been widely employed in fluid flow simulations by several authors (see, for example, *Zienckiewicz and Taylor*, 2000). It is also used in the present work and many numerical simulations performed at the Computational Applied Mechanics Center laboratory of the PPGEC/UFRGS. It is observed that recent advances concerning the FEM are related to reduced numerical integration of element matrices. In this technique the matrices are evaluated analytically and the full quadrature rule may be circumvented by the implementation of an hourglass control algorithm.

Concerning the Taylor time discretization procedures, they can be basically classified in three different methods according to *Yoon et al.* (1998): fully implicit, semi-implicit and fully explicit. Fully implicit algorithms are appropriate in steady state problems and they are also recommended for problems with high nonlinearities and algorithms where the pressure variable is implicitly considered. However, they have an important limitation related to the memory storage, which is very high in large scale simulations. Semi-implicit schemes were created in order to use the main advantages of the fully implicit and fully explicit schemes. Meanwhile, it is observed that the semi-implicit model works well at moderate Reynolds numbers (Re) only. *Braun and Awruch* (2004) have recently studied this model. Although they obtained good results at high Reynolds numbers in a lid-driven cavity analysis, it was later verified that in open boundary flows, such as the flow over an immersed cylinder, the model presented severe stability restrictions even at intermediate Reynolds numbers. Fully explicit schemes are restricted by stability conditions in terms of the time step adopted. Nevertheless, the time step in turbulent flows is intrinsically restricted by physical reasons, so that the main drawback of this model becomes meaningless.

The two-step Taylor-Galerkin model, presented by *Kawahara and Hirano* (1983), is a classical way to solve the governing equations of fluid flows explicitly (*Braun*, 2002). However, in the work presented by *Braun and Awruch* (2004), where a semi-implicit code was used, it was verified that the number of iterations to solve the momentum equation is greater than one only at early stages of the analysis, generally two or three iterations are necessary. Consequently, the two-step method is clearly less economic when it is compared to an iterative-explicit procedure to solve the momentum and energy equations. Hence, the authors suggest a small modification of the algorithm presented by *Braun and Awruch* (2004). In this new algorithm the pressure is solved in an explicit single step instead of an implicit procedure used in the former model. Besides, the components of the pressure gradient are also incorporated in the iterative process of the momentum equation. All the remaining characteristics of the model are maintained. The continuity equation is obtained invoking the pseudo-compressibility hypothesis. Large Eddy Simulation (LES) with the Smagorinsky's sub-grid model is employed in the turbulence modeling. In the non isothermal problem, buoyancy forces, obtained from the classical Boussinesq's approximation, are considered. Eight-node isoparametric hexahedral finite elements are used in the spatial discretization and analytical integration of the element matrices with hourglass control (*Christon*, 1997) is performed.

2. The governing equations of the fluid flow

The governing equations of a non-isothermal incompressible flow of a Newtonian fluid are given by the following expressions:

Momentum equations:

$$\frac{\partial U_i}{\partial t}+\frac{\partial f_{ij}}{\partial x_j}+\frac{\partial p}{\partial x_j}\delta_{ij}-\frac{\partial \tau_{ij}}{\partial x_j}=b_i \qquad (i,j=1,2,3) \quad \text{in } \Omega \tag{1}$$

Mass conservation equation:

$$\frac{1}{c^2}\frac{\partial p}{\partial t}+\frac{\partial U_i}{\partial x_i}=0 \qquad (i=1,2,3) \quad \text{in } \Omega \tag{2}$$

Energy conservation equation:

$$\frac{\partial(\rho u)}{\partial t}+\frac{\partial(\rho u v_i)}{\partial x_i}-\frac{\partial}{\partial x_i}\left[K\frac{\partial u}{\partial x_i}\right]=Q \qquad (i=1,2,3) \quad \text{in } \Omega \tag{3}$$

with

$$U_i=\rho v_i \quad ; \quad f_{ij}=v_j U_i \quad ; \quad \tau_{ij}=\mu\left(\frac{\partial v_i}{\partial x_j}+\frac{\partial v_j}{\partial x_i}\right)+\lambda\frac{\partial v_k}{\partial x_k}\delta_{ij} \quad (i,j,k=1,2,3) \tag{4}$$

where v_i are the velocity components in the direction of the axis x_i, p is the pressure, ρ is the specific mass, u is the internal specific energy, μ is the molecular dynamic viscosity, λ is the volumetric viscosity, c is the sound propagation speed, K is the thermal conductivity constant, Q is the source term and δ_{ij} is the Kroenecker delta. Ω is the domain where the flow is analyzed.

In order to solve the system of differential equations above, it is necessary to define initial conditions and boundary conditions given by:

$$U_i=U_i^p \qquad (i=1,2,3) \qquad \text{in } \Gamma_U \tag{5}$$

$$p=p^p \qquad \text{in } \Gamma_p \tag{6}$$

$$u=u^p \qquad \text{in } \Gamma_u \tag{7}$$

and

$$\left(\tau_{ij}-p\delta_{ij}\right)n_j=t_i \qquad (i,j=1,2,3) \qquad \text{in } \Gamma_\sigma \tag{8}$$

$$K\frac{\partial u}{\partial x_j}n_j=\overline{q} \qquad (j=1,2,3) \qquad \text{in } \Gamma_q \tag{9}$$

where U_i^p, p^p and u^p are prescribed values of U_i, p and u in the parts Γ_U, Γ_p and Γ_u of the total boundary, respectively. $\overline{q}$ and t_i are the boundary flux and the boundary load components in the direction of the axis x_i, respectively, and n_j are the cosine of the angles formed by the normal at a point on Γ_σ or Γ_q with respect to the coordinates system.

In this work the thermal effects over the momentum equations are considered as buoyancy forces according to the Boussinesq's approximation, given by:

$$b_i = \frac{\beta g_i \rho_\infty}{c_v}\left(u - u_\infty\right) \qquad (i = 1,2,3) \tag{10}$$

where β is the volumetric expansion coefficient of the fluid, g_i are the components of the gravity vector acting in the direction of the axis x_i and c_v is the specific heat coefficient at constant volume. ρ_∞ and u_∞ are the reference values of specific mass and internal specific energy, respectively. The energy conservation equation and the body force vector must be disregarded in isothermal problems.

A turbulence closure model must be incorporated in the numerical code if turbulent flows are analyzed. In this work it is used the Large Eddy Simulation (LES) with the Smagorinsky's sub-grid model (*Smagorinsky*, 1963). More details about LES models may be found in *Murakamy* (1997) and *Petry* (2003). In the present model an eddy viscosity (μ_t) must be added to the molecular viscosity μ in the viscous stress tensor. Moreover, a turbulent thermal conductivity is also added to the thermal conductivity in the energy equation. The eddy viscosity, proposed by *Smagorinsky* (1963), is given by:

$$\mu_t = \rho\left(C_S \overline{\Delta}\right)^2 \left|\overline{S}\right| = \rho\left(C_S \overline{\Delta}\right)^2 \left(2\overline{S}_{ij}\overline{S}_{ij}\right)^{1/2} \tag{11}$$

where $\overline{S}_{ij}$ is the strain rate tensor of the fluid, C_S is the Smagorinsky's coefficient ($0.10 \le C_S \le 0.25$) and $\overline{\Delta}$ is a characteristic dimension of the filter. When the Finite Element Method (FEM) is used, element sizes may be considered as filters, separating large and small turbulence scales, and in this case, $\overline{\Delta}^{(e)}$ is given by:

$$\overline{\Delta}^{(e)} = \left(\Omega^{(e)}\right)^{1/3} \tag{12}$$

where $\Omega^{(e)}$ is the volume of the element (e). The overbars are related to the filtered variables.

The turbulent thermal conductivity K_t may be obtained from the following expression:

$$K_t = \frac{\mu_t}{\mathrm{Pr}} \tag{13}$$

where Pr is the Prandtl number.

3. The explicit-iterative Taylor-Galerkin scheme

A modified version of the algorithm presented by *Braun and Awruch* (2004) is implemented in this work. The governing equations are expanded in Taylor series up to second order terms, according to *Yoon et al.* (1998), and the classical Galerkin technique is then applied with the FEM. Equal order shape functions are used for pressure and velocity components approximations at element level. Element matrices are evaluated analytically using one-point quadrature. Hourglass control, similar to that presented by *Christon* (1997), is implemented in order to avoid spurious modes.

The following expressions are obtained after the time discretization:

$$\begin{aligned}\left\{\Delta U_i^{n+1}\right\}^*\Big|_{\mathrm{I}+1} = \Delta t\left(-\frac{\partial f_{ij}}{\partial x_j}^n + \frac{\partial \tau_{ij}}{\partial x_j}^n + b_i^{\,n} - \frac{\partial p}{\partial x_j}^n \delta_{ij} + \frac{\Delta t}{2}\frac{\partial}{\partial x_k}\left[v_k^{\,n}\left(\frac{\partial f_{ij}}{\partial x_j}^n + \frac{\partial p}{\partial x_j}^n \delta_{ij} - b_j^{\,n}\right)\right]\right) + \\ \frac{\Delta t}{2}\left(-\frac{\partial \Delta f_{ij}}{\partial x_j}^n\Bigg|_{\mathrm{I}} + \frac{\partial \Delta \tau_{ij}}{\partial x_j}^n\Bigg|_{\mathrm{I}} + \frac{\Delta t}{2}\frac{\partial}{\partial x_k}\left[v_k^{\,n}\left(\frac{\partial f_{ij}}{\partial x_j}^n - b_j^{\,n}\right)\right]\Bigg|_{\mathrm{I}}\right)\end{aligned} \tag{14}$$

$$\left\{\Delta U_i^{n+1}\right\}^{**} = \frac{\Delta t}{2}\left(-\frac{\partial \Delta p}{\partial x_j}^{n+1}\delta_{ij} + \frac{\Delta t}{2}\frac{\partial}{\partial x_k}\left[v_k \frac{\partial \Delta p}{\partial x_j}^{n+1}\delta_{ij}\right]\right) \tag{15}$$

$$\Delta p^{n+1} = -c^2 \Delta t\left(\frac{\partial U_i}{\partial x_i}^n + \frac{1}{2}\frac{\partial\left\{\Delta U_i^{n+1}\right\}^*\Big|_{\mathrm{I}+1}}{\partial x_i} - \frac{\Delta t}{2}\frac{\partial^2 p}{\partial x_i^2}^n\right) \tag{16}$$

$$\begin{aligned}\Delta\left(\rho u\right)^{n+1}\Big|_{\mathrm{I}+1} = \Delta t\left(-\frac{\partial\left(fu\right)_i^n}{\partial x_j} + \frac{\partial}{\partial x_j}\left[K\frac{\partial u^n}{\partial x_i}\right] + Q^n + \frac{\Delta t}{2}\frac{\partial}{\partial x_k}\left[v_k^{\,n}\frac{\partial\left(fu\right)_i^n}{\partial x_j}\right]\right) + \\ \frac{\Delta t}{2}\left(-\frac{\partial\Delta\left(fu\right)_i^{n+1}\Big|_{\mathrm{I}}}{\partial x_j} + \frac{\partial}{\partial x_j}\left[K\frac{\partial\Delta u^{n+1}\Big|_{\mathrm{I}}}{\partial x_i}\right] + \frac{\Delta t}{2}\frac{\partial}{\partial x_k}\left[v_k^{\,n}\frac{\partial\Delta\left(fu\right)_i^{n+1}\Big|_{\mathrm{I}}}{\partial x_j}\right]\right)\end{aligned} \tag{17}$$

where $(fu)_i = v_i(\rho u)$. Index n and I, are time step and iteration counters, respectively.

The numerical algorithm used in this work may be summarized by the following steps:

1. Compute $\left\{\Delta U_i^{n+1}\right\}^*$ with Eq. (14) using an explicit-iterative process. Observe that a pressure term (which was not considered in *Braun and Awruch*, 2004) is included here;
2. Compute Δp^{n+1} with Eq. (16) using an one-step explicit process;
3. Compute $\left(\Delta U_i^{n+1}\right)^{**}$ with Eq. (15). Incremental pressure terms, omitted in Eq. (14), are included here;
4. Compute $U_i^{n+1} = U_i^n + \left[\left(\Delta U_i^{n+1}\right)^* + \left(\Delta U_i^{n+1}\right)^{**}\right]$;
5. Compute $p^{n+1} = p^n + \left(\Delta p\right)^{n+1}$;
6. If a non-isothermal analysis is performed, compute $\Delta\left(\rho u\right)^{n+1}$ with Eq. (17) using an explicit-iterative process;
7. Compute $u^{n+1} = u^n + \Delta\left(\rho u\right)^{n+1} / \rho$;
8. Return to the first step to initiate the process for a new time interval.

Concerning the numerical algorithm presented above, it was verified that the processing time is significantly reduced when the pressure gradient term, corresponding to the time interval n, is set in Eq. (14) instead of including only increments of the pressure terms in Eq. (15) (*Braun and Awruch* (2004) omitted pressure terms in Eq. (14), using them only in Eq. (15)). Although the time step restrictions ($\Delta t \leq \Delta x / \left(c + V_\infty\right)$, where Δx = element characteristic dimension and V_∞ is the characteristic velocity) become more rigorous when the pressure equation (Eq. 16) is solved explicitly, the processing time and memory requirements are obviously smaller when it is compared to a semi-implicit scheme. In addition, the iterative process to solve the momentum equation of the present model eliminates the need to solve the governing equation twice in each time step as it is performed in the two-step explicit Taylor-Galerkin algorithms (*Kawahara and Hirano*, 1983; *Braun*, 2002).

4. Numerical examples

4.1. Isothermal flows

4.1.1 The 3-D lid-driven cavity

The geometrical characteristics and the boundary conditions used in the cavity analysis are depicted in Fig. 1 - left. Three cases were considered with different Reynolds numbers ($\mathrm{Re} = \rho B u_0 / \mu$) and aspect ratios (B:H:L). Some important parameters related to the cases presented in this work are shown in Tab. 1. The fluid properties employed in the analysis are the following: ρ = 1.0 Kg/m^3, u_0 = 10 m/s, c = 100 m/s and λ = 0. Consequently, the dynamic viscosity is defined according to the Reynolds number as follows: μ = 10/Re. The Smagorinsky's constant is C_s = 0.15 at Re = 10000.

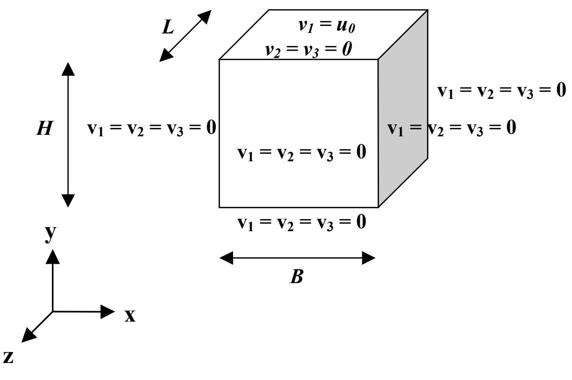

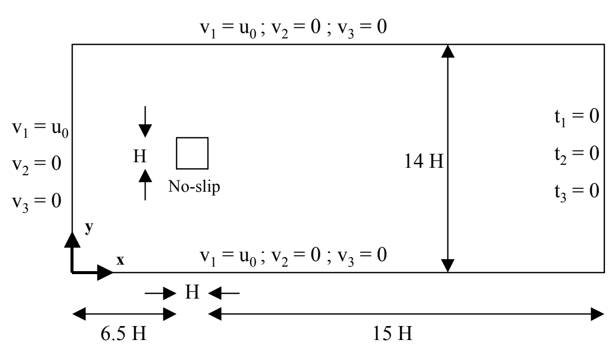

Figure 1. Geometry and boundary conditions; left: 3-D cavity flow and right: flow over a square cylinder

Table 1. 3-D cavity flow: mesh and physical parameters

Case	Re	Aspect Ratio (B:H:L)	Grid Points (x,y,z)	Time increment – Δt [s]
1	1000	1:1:1	(32,32,32)	$1.4\text{x}10^{-4}$
2	3200	1:1:1	(32,32,32)	$1.4\text{x}10^{-4}$
3	10000	1:1:0.25 (simmetry cond.)	(64,64,16)	$7.5\text{x}10^{-5}$

The velocity profiles on the mean plane of the cavity (z = 0.5 and z = 0.25) are presented in Fig. 2. The results are compared to the work of *Tang et al.* (1995) for Re = 10^3 and *Prasad and Koseff* (1989) for Re = $3.2\text{x}10^3$ and Re = 10^4. The last reference is an experimental work. It is important to notice that the results referred to Re = 10^4 are time-averaged values because fluctuations occurs due to turbulence effects. The pressure fields on the mean plane are presented in Fig. 3.

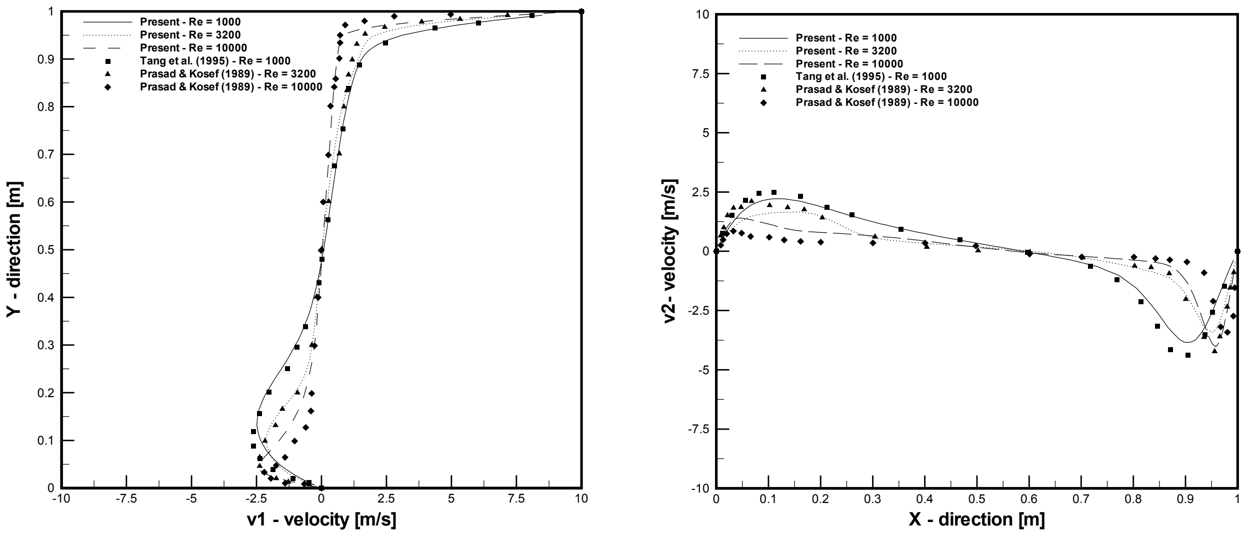

Figure 2. Velocity profiles on the mean plane of the cavity

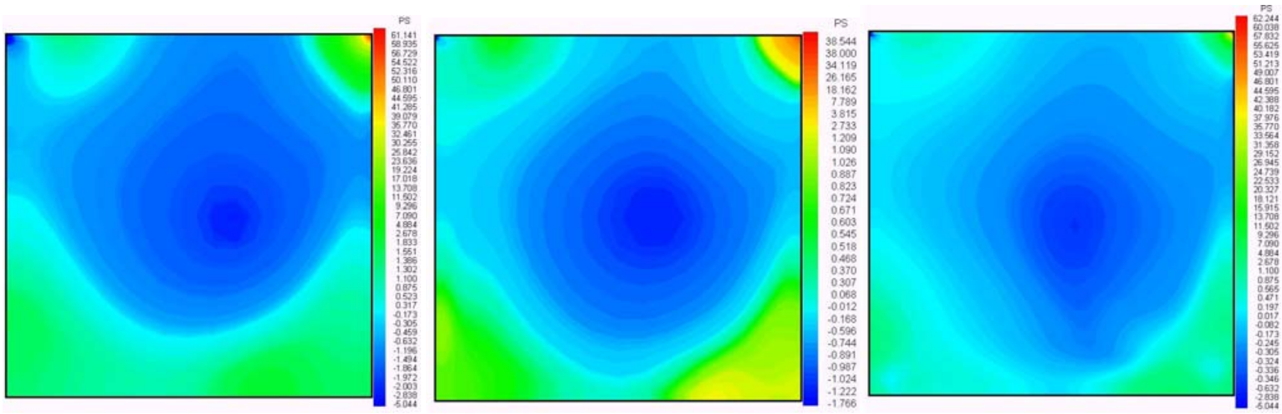

Figure 3. Pressure fields on the mean plane; left: Re = 1000, middle: Re = 3200 and right: 10000

4.1.2 2-D flow over a rectangular cylinder

The geometrical characteristics and the boundary conditions used in the case of a 2-D flow over a square cylinder are presented in Fig. 1 - right. The numerical analysis was performed at a Reynolds number ($\text{Re} = \rho \text{H} u_0 / \mu$) equal to 22000. The fluid properties used in this study are: ρ = 1.0 Kg/m^3, u_0 = 10 m/s, c = 100 m/s, μ = $4.5\text{x}10^{-4}$ and λ = 0. The Smagorinsky's constant is C_s = 0.15. The time-step adopted is $4.0\text{x}10^{-5}$s for a mesh of 31125 elements and 63020 nodes.

Time-averaged aerodynamic results obtained by the present model are compared to those of other authors and summarized in Tab. 2. The aerodynamic coefficients C_D (drag – x direction) and C_L (lift – y direction) are obtained from the evaluation of the expression (8) on the surface of the square cylinder. The force coefficients are normalized with respect to the fluid dynamic pressure at an undisturbed position and the cylinder dimension H. The Strouhal number (St) is defined as $f\text{H}/u_0$, where f is the vortex shedding frequency obtained from the time history of the lift coefficient.

The normalized time-averaged streamwise velocity distribution along the wake centerline is shown in Fig. 4 - left and compared to other works. Finally, Fig. 4 - right shows the time-averaged pressure field and streamlines obtained by the present study.

Table 2. Flow over a square cylinder: aerodynamic results

Work	Aerodynamic results		
	C_D	$(C_L)_{rms}$	St
Present	2.19	1.75	0.142
Lee (1998) – num.	2.15	1.6	0.134
Lyn et al. (1995) – exp.	2.1	-	0.134

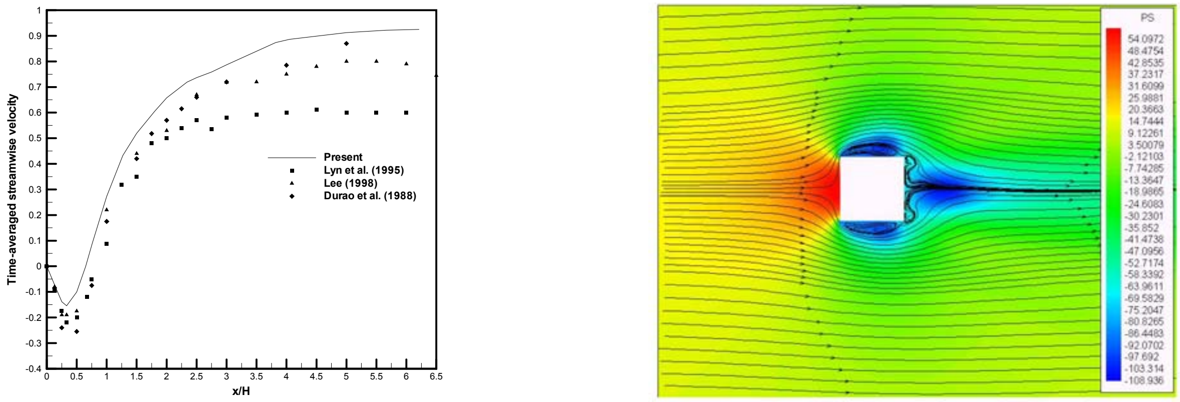

Figure 4. Flow over a square cylinder; left: streamwise velocity profile and right: pressure field and streamlines

4.2. Non-isotheral flows

4.2.1 The 3-D thermal-driven cavity

The natural convection driven by buoyancy forces in a 3-D cubic cavity with unit dimensions is analyzed. No-slip and adiabatic boundary conditions are imposed on the cavity walls, except for the walls perpendicular to the *x*-axis where a unit temperature gradient is prescribed along the *x* direction (see Fig. 1 - left). Two different analyses are performed according to the Rayleigh number ($\mathrm{Ra} = \rho g_i \beta \left(\Delta T\right) L^3 / \mu K$, where L = characteristic dimension): Ra = 1.0x10^4 and Ra = 1.0x10^6. The Prandtl number is kept equal to one in both simulations. The mesh used in the analyses contains 38x38x38 elements. The time step used in both examples is equal to 1.0x10^{-3} s.

Results referred to temperature and velocity profiles on the mid plane (y = 0.5) of the cavity are presented in Fig. 5. An excellent agreement with *Wong and Baker* (2002) is observed.

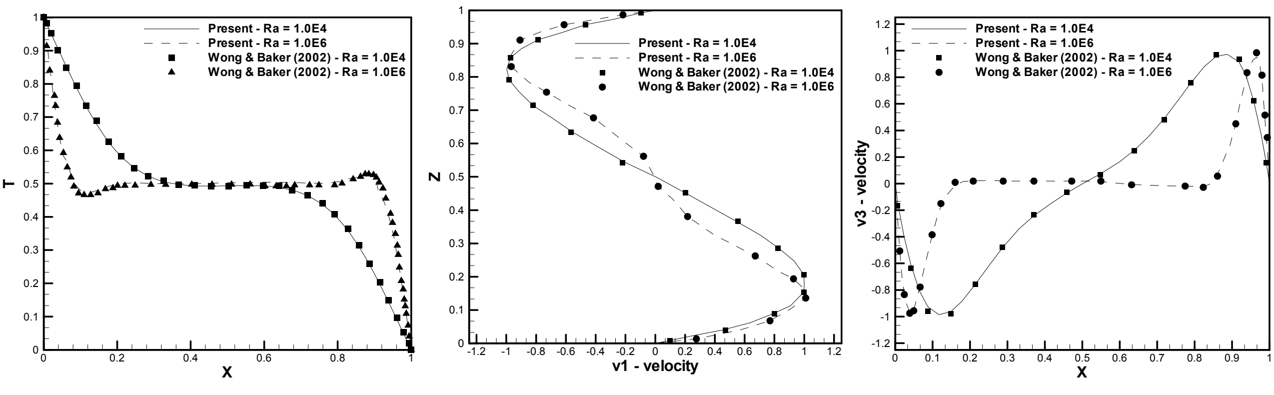

Figure 5. Thermal-driven cavity flow; left: temperature profile, middle: v_1 velocity profile and right: v_3 velocity profile

4.2.2 2-D flow over a heated/cooled circular cylinder

Thermal effects over the vortex shedding phenomenon around a 2-D circular cylinder is analyzed. The geometrical domain and the boundary conditions are illustrated in Fig. 6. Five different situations are studied according to the Richardson number ($\mathrm{Ri} = g_i \beta \left(\Delta T\right) D / V_\infty$ where V_∞ is the characteristic velocity): Ri = - 1.0, Ri = - 0.5, Ri = 0.0, Ri = 0.5 and Ri = 1.0. The Prandtl and Reynolds numbers are chosen to be equal to 0.71 and 100, respectively, in all simulations. The mesh is constituted by 6800 elements and 13980 nodes and the time step is equal to 1.0x10^{-4} s.

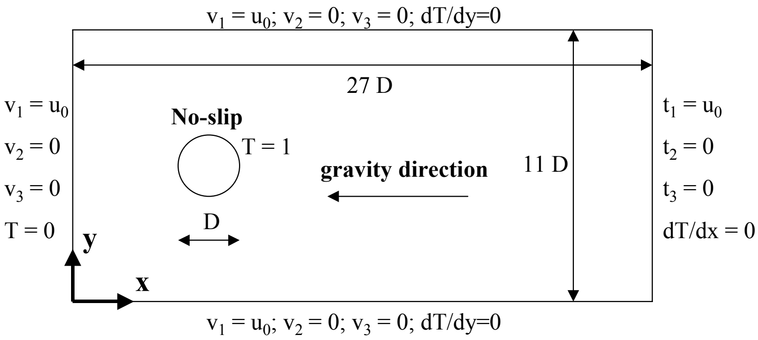

Figure 6. Non-isothermal flow over a 2-D circular cylinder: domain and boundary conditions

Results related to temperature fields and streamlines for the five cases studied here are presented in Fig. 7. As it can be noticed, negative range of the Richardson number are characterized by a well-defined vortex street, which gets narrower as the Richardson number increases. Increasing the Richardson number from zero to one, the vortex street disappears and the flow becomes steady with two static vortices behind the cylinder, which get smaller as the Richardson number increases owing to the buoyancy forces that push downstream the separation points.

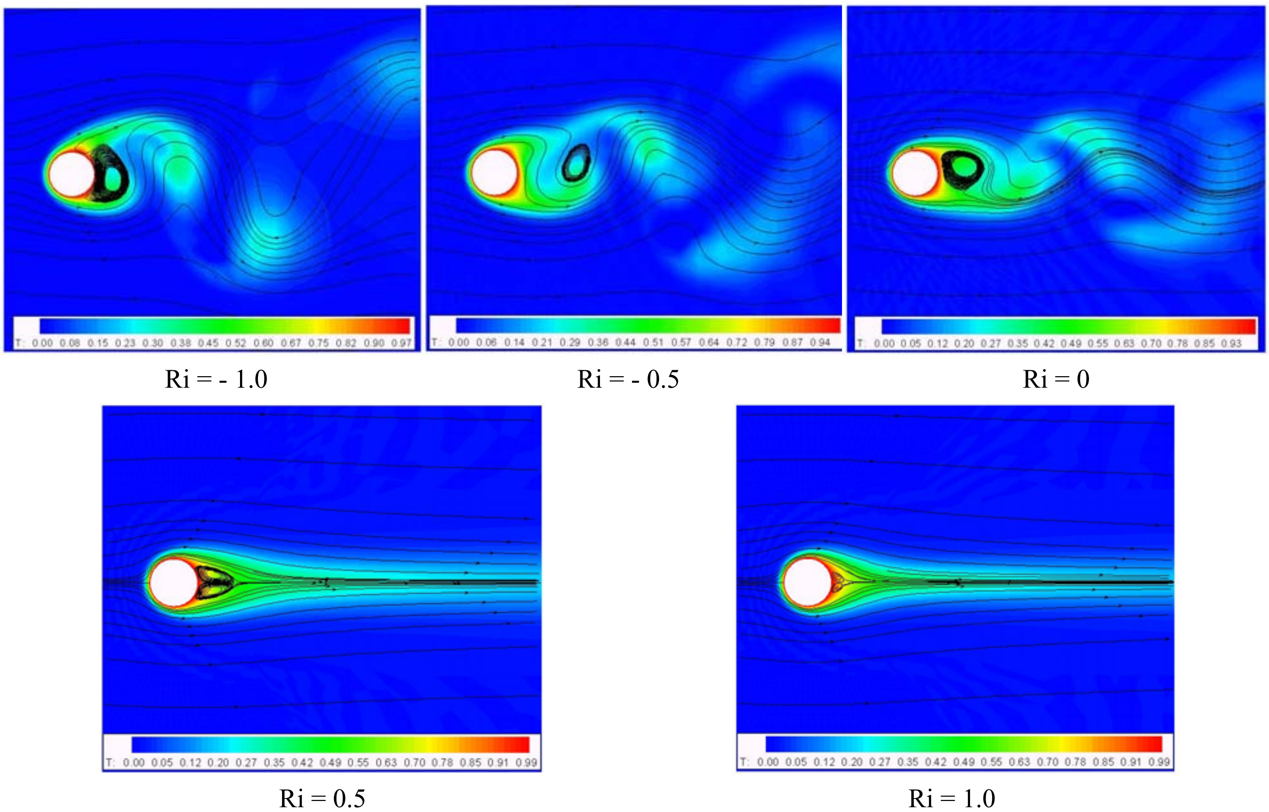

Figure 7. Isothermal fields and streamlines according to the Richardson number

Finally, results referred to the Strouhal number (St) are present in Tab. 3. They are compared to the numerical work by *Hatanaka and Kawahara* (1995).

Table 3. Strouhal number according to the Richardson number

Work	Strouhal number (St)				
	Ri = -1.0	**Ri = -0.5**	**Ri = 0**	**Ri = 0.5**	**Ri = 1.0**
Present	0.110	0.154	0.181	-	-
Hatanaka & Kawahara (1995)	0.100	0.150	0.175	-	-

5. Conclusions

An explicit-iterative algorithm to solve isothermal and non-isothermal incompressible flows was presented in this paper. As it was expected, the iterative procedures to solve the momentum and energy equations presented a single iteration in most of the numerical process. The convergence rate was enhanced setting the pressure gradient term in the iterative process of the momentum equation (Eq. 14). The numerical model was able to simulate *CFD* (*Computational Fluid Dynamics*) classical examples. Turbulent flows were studied successfully, where the same characteristics related to the efficiency of the numerical solver were also observed. The thermal effects over the flow characteristic were correctly simulated and the aerodynamic parameters of the immersed bodies, such as force coefficients and Strouhal numbers, were obtained in agreement with other works. Hence, the model proved to be an efficient and accurate numerical algorithm to analyze large-scale problems. In future works it is expected to use the present model in applications to *Computational Wind Engineering* (*CWE*) problems.

6. Acknowledgements

The authors would like to thank to CNPQ for the financial support.

7. References

Braun, A.L., 2002, "A Numerical Model for the Simulation of the Wind Action over Bridge Cross-Sections" (In Portuguese), MSc Thesis, Graduate Program in Civil Engineering / Federal University of Rio Grande do Sul (PPGEC/UFRGS), Porto Alegre, Brazil.

Braun, A.L. and Awruch, A.M., 2004, "A segregated scheme for turbulent incompressible flows simulation", In: XXV CILAMCE – Iberian Latin American Congress on Computational Methods in Engineering, Recife – PE, Brazil.

Braun, A.L. and Awruch, A.M., 2005, "Aerodynamic and aeroelastic analysis of bundled cables by numerical simulation", Journal of Sound and Vibration, Vol. 284, n° 1-2, pp. 51-73.

Christon, M.A., 1997, "A domain-decomposition message-passing approach to transient viscous incompressible flow using explicit time integration", Computer Methods in Applied Mechanics and Engineering, Vol. 148, pp. 329-352.

Durao, D.F.G.; Heitor, M.V. and Pereira, J.C., 1998, "Measurements of turbulent and periodic flows around a square cross-section cylinder", Experimental Fluids, Vol. 6, pp. 298-304.

Hatanaka, K. and Kawahara, M., 1995, "A numerical study of vortex shedding around a heated/cooled circular cylinder by the three-step Taylor-Galerkin Method", International Journal for Numerical Methods in Fluids, Vol. 21, pp. 857-867.

Kawahara, M. and Hirano, H., 1983, "A finite element method for high Reynolds number viscous fluid flow using two step explicit scheme", International Journal for Numerical Methods in Fluids, Vol. 3, pp. 137-163.

Murakami, S., 1997, "Current status and future trends in computational wind engineering", Journal of Wind and Industrial Aerodynamics, Vol. 67&68, pp. 3-34.

Lee, S., 1998, "Numerical study of wake structure behind a square cylinder at high Reynolds number", Wind and Structures, Vol. 1, n°2, pp. 127-144.

Lyn, D.A.; Einav, E.; Rodi, W. and Park, J.H., 1995, "A laser-Doppler velocimeter study on ensemble-averaged characteristics of the turbulent near wake of a square cylinder", Journal of Fluid Mechanics, Vol. 304, pp. 285-319.

Petry, A.P., 2002, "Numerical Analysis of 3-D Turbulent Flows Using the Finite Element Method and Large Eddy Simulation" (In Portuguese), DSc. Thesis, Graduate Program in Civil Engineering / Federal University of Rio Grande do Sul (PPGEC/UFRGS), Porto Alegre, Brazil.

Prasad, A.K. and Koseff, J.R., 1989, "Reynolds number and end-wall effects on a lid-driven cavity flow", Physics of Fluids A, Vol. 1, pp. 208-219.

Smagorinsky, J., 1963, "General circulation experiments with the primitive equations I, the basic experiment", Monthly Weather Review, Vol. 91, pp. 99-165.

Tang, L.Q.; Cheng, T. and Tsang, T.T.H., 1995, "Transient solutions for three-dimensional lid-driven cavity flows by a least-squares finite element method", International Journal for Numerical Methods in Fluids, Vol. 21, pp. 413-432.

Wong, K.L. and Baker, A.J., 2002, "A 3D incompressible Navier-Stokes velocity-vorticity weak form finite element algorithm", International Journal for Numerical Methods in Fluids, Vol. 38, pp. 99-123.

Yoon, K.T.; Moon, S.Y.; Garcia, S.A.; Heard, G.W. and Chung, T.J., 1998, "Flow field-dependent mixed explicit-implicit (FDMEI) methods for high and low speed and compressible and incompressible flows", Computer Methods in Applied Mechanics and Engineering, Vol. 151, pp. 75-104.

Zienckiewicz, O.C. and Taylor, R.L., 2000, "The Finite Element Method – 5th Ed.", Butterworth-Heinemann, Oxford, UK.

8. Responsibility notice

The authors are the only responsible for the printed material included in this paper.